ELSEVIER

Surface Science 500 (2002) 500–522

SURFACE SCIENCE

www.elsevier.com/locate/susc

The growth and modification of materials via ion–surface processing

Luke Hanley [a,*], Susan B. Sinnott [b]

[a] *Department of Chemistry, The University of Illinois at Chicago, Chicago, IL 60607-7061, USA*
[b] *Department of Materials Science and Engineering, The University of Florida, 100 Rhines Hall, Gainesville, FL 32611, USA*

Received 12 July 2000; accepted for publication 31 January 2001

Abstract

A wide variety of gas phase ions with kinetic energies from 1–10^7 eV increasingly are being used for the growth and modification of state-of-the-art material interfaces. Ions can be used to deposit thin films; expose fresh interfaces by sputtering; grow mixed interface layers from ions, ambient neutrals, and/or surface atoms; modify the phases of interfaces; dope trace elements into interface regions; impart specific chemical functionalities to a surface; toughen materials; and create micron- and nanometer-scale interface structures. Several examples are developed which demonstrate the variety of technologically important interface modification that is possible with gas phase ions. These examples have been selected to demonstrate how the choice of the ion and its kinetic energy controls modification and deposition for several different materials. Examples are drawn from experiments, computer simulations, fundamental research, and active technological applications. Finally, a list of research areas is provided for which ion–surface modification promises considerable scientific and technological advances in the new millennium.

Keywords: Ion–solid interactions; Growth; Ion etching; Ion bombardment; Ion implantation; Sputtering; Computer simulations; Molecular dynamics

1. Overview and motivation

The development of new materials continues to be one of the ongoing technological and scientific revolutions at the dawn of the 21st century. Interface science is at the forefront of this revolution because surfaces of materials dictate many of their most important properties. Continuing progress in many technological applications requires the engineering of interfaces with a wide range of chemical, physical, and/or morphological characteristics.

A wide variety of gas phase ions with kinetic energies from 1–10^7 eV increasingly are being used for the growth and modification of state-of-the-art material interfaces. Ions can be used to deposit thin films; expose fresh interfaces by sputtering; grow mixed interface layers from ions, ambient neutrals, and/or surface atoms; modify the phases of interfaces; dope trace elements into interface

* Corresponding author. Tel.: +1-3129960945; fax: +1-3129960431.
E-mail addresses: lhanley@uic.edu (L. Hanley), sinnott@mse.ufl.edu (S.B. Sinnott).

0039-6028/01/$ - see front matter
PII: S0039-6028(01)01528-X

regions; impart specific chemical functionalities to a surface; toughen materials; and create micron- and nanometer-scale interface structures. Ion-induced processes allow the engineering of interfaces with specific wettability, hardness, resistance to corrosion, optical parameters, electronic functionality, dimensionality, and/or biocompatibility. Technologically important ion–surface processes include the production of hard coatings for machine tools and computer disk drives; biocompatible surfaces for tissue culture, contact lenses, medical implants, and other biomedical devices; antireflective and protective optical coatings; polymer films for packaging and adhesives; combinatorial arrays; and chemical sensors. Current or potential steps of microelectronics manufacturing that involve ion–surface modification include reactive ion etching, ion beam repair of photolithography masks, doping of semiconductors, and development of commercially viable sub-100 nm ion projection lithography.

Its versatility puts ion–surface modification at the center of a wide range of fundamental research. Not only can interface properties be adjusted experimentally via ion–surface interaction, but experimental data can be supplemented by an array of computational methods that accurately model those interactions. Ion–surface collisions also play an important role in other interface modification methods that might be considered unrelated at first glance, including plasma processing and pulsed laser deposition. However, the collision between a specific ion of a given kinetic energy with a surface can be readily modeled by computer simulations. By contrast, plasmas, sputter plumes, and laser plumes involve multiple particles with broad energy distributions that can only be simulated by correspondingly more complex computer models. Few interface modification methods possess computer modeling tools as powerful and accurate as those afforded to ion–surface modification.

Unlike neutrals, ions can be easily accelerated to any kinetic energy between 1 and 10^7 eV. The amount of energy imparted to a surface or buried interface region of a material is readily controlled by varying this kinetic energy. The chemical and physical processes that are induced in the surface by ion impact also are controlled by this kinetic energy [1–8]. A specific terminology has arisen to define approximate ion energy ranges: ion kinetic energies <1 eV are known as thermal, 1–500 eV are hyperthermal, 0.5–10 keV are low energy, 10–500 keV are medium energy and >0.5 MeV are high energy.

Fig. 1 displays how ion–surface processes vary with kinetic energy. Thermal ions can physisorb or chemisorb on the surface, dissociate and chemisorb to the surface (activated dissociative chemisorption), or simply scatter off the surface with some loss in their kinetic energy (direct inelastic scattering). Hyperthermal ions additionally can abstract atoms from surfaces (abstraction reactions) or dissociate and scatter if they are polyatomic (dissociative scattering). The ions also may react with the substrate atoms to create altogether new chemical species. These new chemical species may be volatile or readily sputtered, leading to surface etching (reactive ion etching). The ions may directly react with the surface atoms to form new species (i.e., oxide/nitride growth). Low energy ions can implant into the surface to form an alloy or doped material (ion implantation).

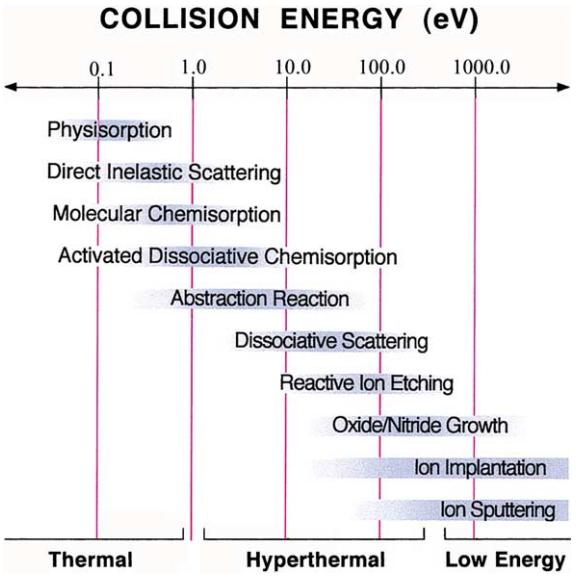

Fig. 1. Fundamental molecule/surface processes: Each shaded region designates the ion kinetic energy range over which the associated process is studied. Adapted from Ref. [150].

Hyperthermal and low energy ions deposit their kinetic energy solely into the surface without affecting the bulk region. This energy deposition causes sputtering of surface atoms as ions or neutrals, annealing of the surface, mixing of surface atoms, creation of unique surface topologies, and defect formation. Low energy ions also can induce secondary collisions of substrate atoms which cause collision cascades and result in energy transfer far from the initial impact point. The effects of low energy ion–surface impacts have been extensively studied by researchers in the field of secondary ion mass spectrometry, where the sputtered ions are used for surface chemical analysis [9,10]. The effects of the impacting ion migrate further into the bulk region of the substrate and away from the impact point with increasing ion energy. As the ion energy increases into the medium and high energy range, the ion–surface interaction moves from predominantly a nuclear–nuclear collision between projectile and target to one that is primarily electronic in nature [11].

A variety of charge transfer processes occur for ion–surface collisions across the full range of incident ion energies. These are not covered in this paper due to their complexity and considerable diversity [5]. It is often assumed that ions simply neutralize at a surface, with little additional effect upon the modified surface beyond the ballistic and chemical effects of the ion. This is often a good assumption for hyperthermal and higher incident ion energies, where the few eV change in energy due to neutralization is relatively insignificant. However, ion impacts at insulating surfaces can lead to charging and alteration of the impact energies or flux of subsequent ions. Also, ion-induced secondary electron emission is a significant process that can cause additional modification of the surface region of polymers, organic films, and other materials [12].

Energy transfer, interface chemical reactions, and other phenomena synergistically combine to make ion–surface modification an extremely versatile method. The chemical and physical processes that are induced in the surface by the ion also are influenced by its chemical identity. A beam of ions of a given chemical identity can be readily prepared by mass selection for subsequent surface interaction. If the ion is polyatomic and impacts with sufficiently low energy, it may attach intact and thereby transfer its chemical functionality to the interface. However, polyatomic ions with kinetic energies far in excess of those required to completely fragment interact differently with a surface than their energy scaled atomic constituents [10,13]. A range of interface chemistries and structures can be imparted through the selection of a projectile ion for its elemental identity, chemical structure, and number of constituent atoms. This modification can be selected for the interface while preserving the native properties of the bulk substrate.

The incredible flexibility of ion–surface modification has been implemented in a wide range of techniques and industrial tools. These are described schematically in Fig. 2. Ion beam synthesis, ion beam deposition, ion beam sputtering, ion beam sputter deposition, ion beam assisted deposition, dual ion beam sputtering, magnetron sputtering, electron beam ion assisted deposition, chemical assisted ion beam etching, reactive ion beam etching, pulsed laser deposition, plasma processing, plasma immersion, ion implantation, intense pulsed ion beams, ionized plasma vapor deposition, physical vapor deposition, and filtered arc deposition all employ ions—at least in part—to modify material interfaces (see Fig. 2 for definitions of these terms) [1,2,6,14–20]. The role of energetic ions is often critical in films grown by these various processes. Ion beam tools are also widely used in semiconductor processing [21] and are under consideration for sub-100 nm lithography [22,23].

Computationally, ion–surface interactions are studied using a variety of methods. One popular computational method is molecular dynamics, an atomistic approach where Newton's second law of motion is solved quantitatively to determine the response of atoms to the forces that are applied to them [24]. The strengths of this method include its ability to model both dynamical and non-equilibrium events. Its main weakness is that it is limited to short time scales on the order of a few picoseconds or nanoseconds. However, this does not prevent molecular dynamics from being used to study ion–surface interactions as the time scales of

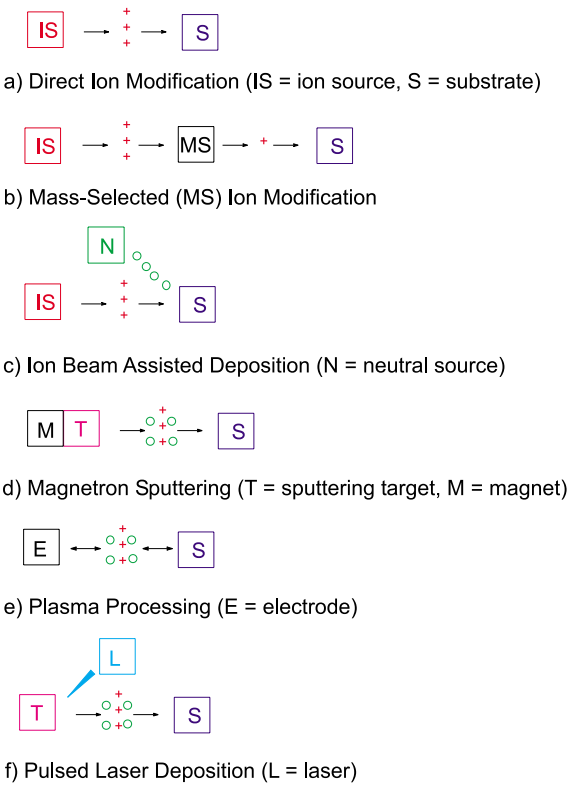

Fig. 2. Schematic diagrams of several general experimental configurations in which ion–surface modification is either central or plays an important role. (a) Direct ion modification involves simply an ion source (IS) to deposit ions (+) on a substrate (S). (b) Mass-selected ion modification filters out ions of a single mass-to-charge ratio for deposition on the surface. Ion beam synthesis, ion beam deposition, ion beam sputtering, ion beam sputter deposition, reactive ion beam etching, and dual ion beam sputtering are all varieties of direct or mass-selected ion modification. (c) Ion beam assisted deposition simultaneously adds a source of neutral species (○), to deposit additional material or provide a reagent for ion-induced chemistry. Two variants on this method are electron beam ion assisted deposition and chemical assisted ion beam etching. (d) Magnetron sputtering uses a magnetically confined discharge to sputter ions and neutrals from a target (T) onto S. The discharge here and in plasma processing is established by a direct or alternating voltage difference applied between T and S. (e) Plasma processing uses the gas feed into the chamber to establish the discharge, with (hopefully) no sputtering of the electrode. Plasma immersion ion implantation, intense pulsed ion beams, ionized plasma vapor deposition, physical vapor deposition and filtered arc deposition are all types of plasma processing that utilize different electrode geometries (i.e., separate second electrode used instead of substrate) and/or electrical waveforms for generating the plasma. (f) Pulsed laser deposition employs a pulsed laser (L) to ablate a target material and thereby eject a plume of neutrals and ions for deposition onto S. All types of ion–surface modification typically occur in a vacuum system with an operating pressure of $\leqslant 10^{-4}$ torr and an input of a feed gas for the ion gun (or discharge) into the chamber (not shown). The ion energy is defined by the voltage difference between the ion source and substrate (not shown). Amongst the wide variety of ion sources used are electron impact, discharges, thermionic, plasmas, supersonic expansion, laser ablation and combinations thereof (often with magnetic confinement) [6]. Configurations (a) through (f) are often supplemented by one or more experimental probes to structurally and/or chemically analyze the interface region following ion modification.

these collisions are typically on the order of a few picoseconds.

Modeling ion–surface interactions with atomistic simulations such as molecular dynamics requires careful consideration of the method or potential used to calculate the energies, and therefore the forces, acting on both the ions and the surfaces. The potential used depends on the nature of the ion's interaction with the surface, which, in turn, depends significantly on the ion's energy. For

example, ions with several eV energy tend to chemisorb or physisorb on the surface. This adsorption can be modeled using empirical and semiempirical potentials that are fit to experimental data and are used to determine atomistic system energies and forces [25–28]. More accurate methods are developed from first principles [29], or model the atoms quantum mechanically but use empirical methods to model interatomic interactions [30]. These same methods can be used for impacts at higher energies where the ions penetrate and disrupt the surface and/or dissociate if they are polyatomic.

At incident energies of around 10 keV, the binary collision approximation is usually used. This method assumes a series of two-body encounters between the ion and atoms in the substrate. The elastic scattering interactions are modeled with repulsive interatomic potentials while inelastic interactions are modeled with potentials that assume electronic excitation has occurred. While the binary collision approximation has found success in modeling high energy processes, recent simulations suggest that many-body methods are more exact [31]. Finally, electronic stopping is dominant in collisions at energies of about 1 MeV, requiring the use of methods that either treat the electrons in the system explicitly or are derived from such methods [32].

Ion–surface interactions also are modeled with atomistic Monte Carlo simulation methods [6,11, 33]. The most popular of the computer codes that implement these methods for ion–surface collisions is known as TRIM (transport of ions in matter), although a variety of related computer codes have evolved from the original TRIM [34]. Monte Carlo simulation methods compare the energy of a proposed new configuration to that of the original configuration using the same methods to calculate energies listed above. If the new configuration is lower in energy it is accepted automatically. However, if the new configuration is higher in energy a random number is used to determine whether or not to accept it. The strength of this method is that it relatively quickly reaches the equilibrium geometry for the system under study, such as a thin film that has been deposited from incident ions. Its weakness is that no dynamical information is available. Sometimes computational approaches use a combination of molecular dynamics and Monte Carlo methods to model ion deposition of thin films. This is usually accomplished by using molecular dynamics to model the ion impacts and Monte Carlo simulation steps to model the relaxation of the system prior to the deposition of the next ion in the beam.

Non-atomistic phenomenological models are also used to characterize the cumulative effects of ion deposition. For instance, semiquantitative models are used that rely on mathematical expressions to keep track of the various processes that can occur during ion–surface interactions and their probabilities. These models are used to determine penetration, adhesion, and defect formation for low energy ion bombardment of surfaces as a function of the reaction conditions [35–37]. The strength of this approach is that after the model has been applied and the results compared to experimental data, information on which ion–surface interactions are most important in producing a given thin film is available. Its weakness is that the model might represent an unphysical conclusion that nevertheless matches experimental data. Additional mathematical models focus on sputtering rather than thin-film growth [7,9].

2. Examples

Several examples are used to demonstrate the variety of technologically important interface modification that is possible with gas phase ions. These examples have been selected to demonstrate how the choice of the ion and its kinetic energy controls modification and deposition for several different materials. However, the wide breadth of the field dictates that these few examples do not fully cover the entire range of ion–surface modification.

2.1. Thin-film growth and chemical modification

2.1.1. Hard carbon nitride film growth

Ion–surface collisions play an important role in the production of mechanically hard films [38]. Theoretical calculations predict that a specific

phase of carbon nitride, β-C_3N_4, is harder than diamond and displays similarly high thermal conductivity [39]. The many potential applications for such a material have encouraged the materials science community to synthesize either β-C_3N_4 or some other variety of hard carbon nitride film. Some of the attempts to produce β-C_3N_4 films utilize mass-selected hyperthermal or low energy ions by codeposition of C^+ and N^+, implantation of N^+ or N_2^+ into graphite or diamond, or codeposition of C_2^- and CN^- [40–44]. The resulting carbon nitride films typically display differing morphologies, mixed phases, and varying C/N ratios. Analytical modeling of the ion beam growth of carbon nitride provides insight about the competition between the processes that lead to thin-film formation—deposition, implantation, diffusion, and densification—and the sputtering and damage to the film from the energetic ions [36]. Magnetron sputtering (see Fig. 2) of graphite targets with nitrogen/argon gas mixtures also may be applied to grow β-C_3N_4 films [40,45,46]. Films grown from magnetron sputtering with a substrate bias of −300 eV are both hardest and smoothest, although they are not of the desired β-C_3N_4 phase [46]. Since the substrate bias causes the acceleration of ions, it is clear that a hyperthermal ion energy is important to growth of high quality carbon nitride films. Magnetron sputtering is now used by many manufacturers to grow hard carbon nitride films on hard disk drive surfaces, improving hard disk lifetimes by reducing wear from the read/write heads [44,46]. Formation of high quality, single phase, crystalline β-C_3N_4 remains a controversial topic, although recent advances are moving closer to this goal [47]. Nevertheless, the commercial success of hard carbon nitride films in hard disk drives remains an important vindication of ion-based film growth methods.

2.1.2. Metal thin films

The controlled growth of metallic thin films is important for the production of a variety of electronic devices such as transistors. Because the metal needs to cover areas on the order of a few micrometers, conventional deposition techniques, such as electroplating, cannot be used. The preferred method of deposition is currently magnetron sputtering. However, this method is not precise enough to be used for contacts on the nanometer scale, which are becoming increasingly important as the size of electronic devices continues to decrease. Two methods that show promise for the production of metallic films with the needed precision are metal ion beam deposition and metal cluster beam deposition.

The quality of metal films produced through metal ion deposition depends on several factors, as indicated schematically in Fig. 3 [5]. The most important is the incident energy which is usually on the order of several eV. Other important factors

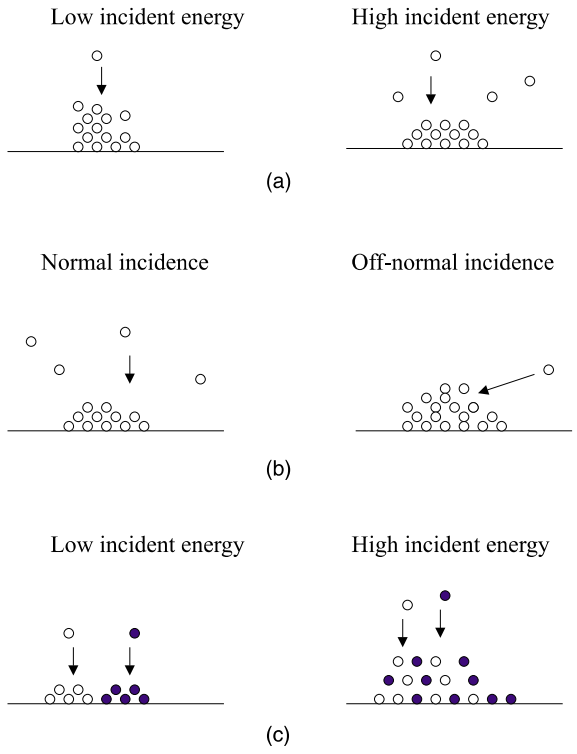

Fig. 3. Schematic showing the various processes that can occur for metal ion deposition. Panel (a) shows how deposition at low incident energy leads to the formation of rough thin films while deposition at higher incident energies yields smoother films but also leads to an increase in sputtering. Panel (b) shows how deposition at normal incidence leads to the formation of smoother films than deposition at an off-normal angle but that the amount of sputtering is higher at normal incidence. Panel (c) compares the deposition of mixed films at low and high incident energies. The degree of mixing and smoothness of the film increases with energy.

are the crystal structure of the surface, the incident angle, and the relative densities of the incident ion and the surface atoms. As the incident energy increases, the deposited ions have enough energy to preferentially diffuse such that layer-by-layer growth is achieved if this is thermodynamically preferred for the system in question. In contrast, very low energies generally yield thin films with significant surface roughness [48]. Combined molecular dynamics and Monte Carlo simulations provide details about the diffusion and coalescence of islands during deposition to form single layers and how these processes change with variations in reaction conditions [49]. For example, the simulations show how intermixing between disparate layers occurs when the incident metal ions are different from the metal substrate, and how this intermixing increases with incident energy. Surface roughness and the shapes of the structures formed also increase in magnitude if the deposition angle increases from the normal [50]. This is due to long-range interactions between the incident ions and the surface, called steering, that become increasingly important at large angles. Steering causes the ions to deposit preferentially on top of islands rather than at island edges, which accounts for the roughness of the surface. Sputtering of the surface is a side effect of metal ion deposition. As expected, the amount of sputtering increases as the ion's kinetic energy goes up but decreases with increasing angles from the surface normal [51].

It should be noted that when metal ions are deposited with energies in the tens of keV range, collision cascades are created within the material that cause local melting [52]. When the molten metal cools, nanometer-scale amorphous regions and defect clusters form within the bulk [53]. This is especially apparent when heavier ions impact a less dense metal substrate. Interstitial point defects and islands can also result [54]. Thus, these high energy bombardments create unique nanostructures and defects near the surface with unusual properties.

The deposition of metallic thin films from clusters is well studied because of the unique properties of cluster beams compared to atomic ion beams [55]. These include the large concentration of atoms and energy that is deposited in a localized region of the surface that facilitates thin-film growth and at the same time causes increased surface damage and sputtering. However, except under extreme conditions, clusters do not penetrate as deeply as single atoms because of their large size [56]. Thus, they have the ability to modify selectively a shallower region of the surface than single ion beams. Despite these benefits, there are experimental problems producing clusters in a reliable manner and verifying their size distribution [57].

One dependable method for depositing metal clusters is with a combination of a magnetron sputter discharge and a gas aggregation source [58]. Deposition conditions include relatively low temperatures of about 500 K and high kinetic energies of 10 eV/atom for clusters of several thousand atoms [59–61]. Thin films grown using this method are smoother than comparable films formed by evaporated deposition and have a dense "mirror-like" finish and good adhesion to a variety of substrates. This process is modeled with molecular dynamics simulations. The top four panels of Fig. 4 contains snapshots from a simulation where a 2000 atom Cu cluster is deposited on a Cu surface with 10 keV of energy [62]. Immediately after impact, a temperature of several 1000 K and a pressure of 80 GPa is produced at the contact area. This pressure pulse is the driving force for a shear process that forms a surface crater. However, the uphill shear motion is impeded by the additional surface atoms so the crater rim formation is suppressed. In the opposite direction there is no such obstacle which allows the rim to slip downhill. The high pressures and temperatures cause an alloying of the substrate with the deposited material leading to a strong adhesion of the coating.

In contrast, highly disordered, porous structures are formed if lower incident energies are used. An example of such a film is shown in the bottom panel of Fig. 4. In this case, a beam of Cu clusters containing 1000 atoms each are deposited on a Cu surface with 10 eV of energy (leading to so-called soft landings) in molecular dynamics simulations [63]. The resulting film exhibits dendritic growth with high roughness, low density and poor adhesion to the substrate. These predictions agree with

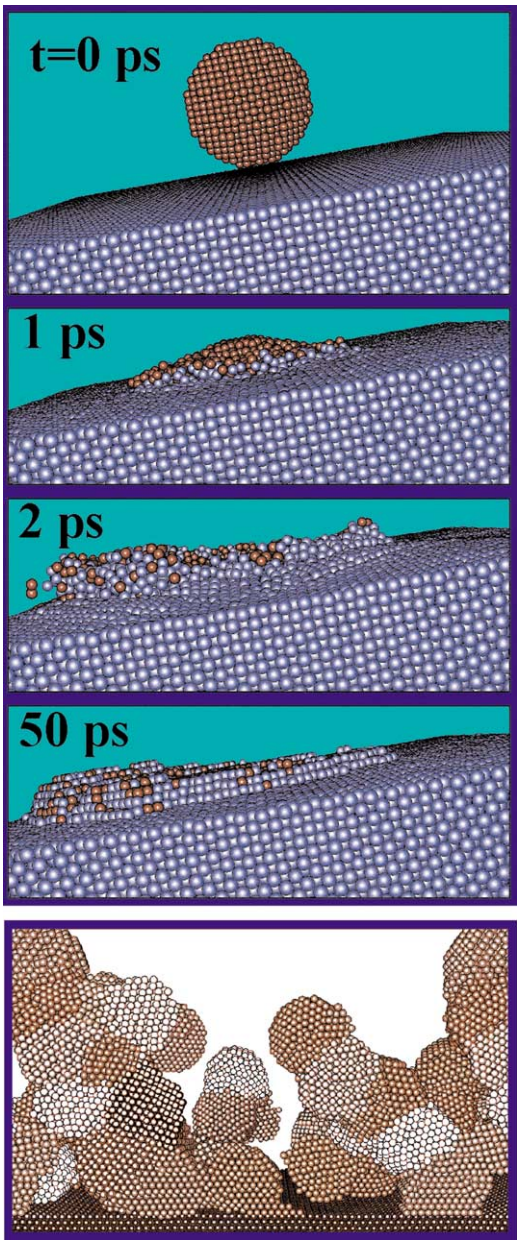

Fig. 4. The top four panels show snapshots from a molecular dynamics simulation of a 2000 atom Cu cluster (red spheres) impinging onto a tilted Cu(0 0 1) surface (blue spheres) at 10 keV of energy. Each panel is labeled with the time from initial contact of the cluster with the surface. The bottom panel shows the final snapshot from a molecular dynamics simulation of a beam of 1000 atom Cu clusters with 10 eV kinetic energy depositing onto a Cu(0 0 1) surface. Note how the quality and character of the films change dramatically with incident cluster energy. Figure used with permission of Elsevier [62,63].

the results of experiments that use laser vaporization to produce smaller (5–10 atoms/cluster) charged and neutral metal clusters that impact with thermal or hyperthermal energies. These experiments reveal that the clusters keep their shape after deposition giving rise to unusual nanostructured films [64].

Atomistic simulations [65–68] shed light on additional ways in which changes in the reaction conditions lead to fundamentally different thin films. For example, they show that smaller clusters (of a few atoms) are more likely to embed themselves into the surface while larger clusters (of more than 50 atoms) are more likely to spread across the surface. In the case of deposition on a surface composed of a different material, they provide information on the way in which the outcome depends on the relative cohesive energies, chemical properties, and atomic masses of the clusters and surfaces. For example, Al does not penetrate Ni because of the mass difference but instead spreads epitaxially, while Ni clusters easily penetrate and embed themselves into Al surfaces. Finally, at high enough impact energies of a few eV/atom, simulations have shown that excitation of electrons is more likely to occur during the early stage of the cluster contact with the surface when the cluster is highly compressed. These core-excited atoms decay by Auger emission following scattering off the surface [32].

2.1.3. Organic thin-film deposition and chemical modification

Hyperthermal atomic ions can be used to chemically modify surfaces or deposit thin films [2]. Small polyatomic ions can induce selective chemical modification of polymer and semiconductor surfaces [69,70]. Certain polyatomic ions land as intact species upon fluorocarbon surfaces at $\sim$10 eV collision energies [71,72]. Polymeric films for applications in optoelectronics can even be grown from organic ion sources [73].

Chemical modification by polyatomic, organic ions can be quite selective, with strong dependence upon the ion structure and kinetic energy [74,75]. Fig. 5 displays the chemical composition of fluorocarbon films grown on a polystyrene surfaces from 25–100 eV CF_3^+ and $C_3F_5^+$ ions. Each ion

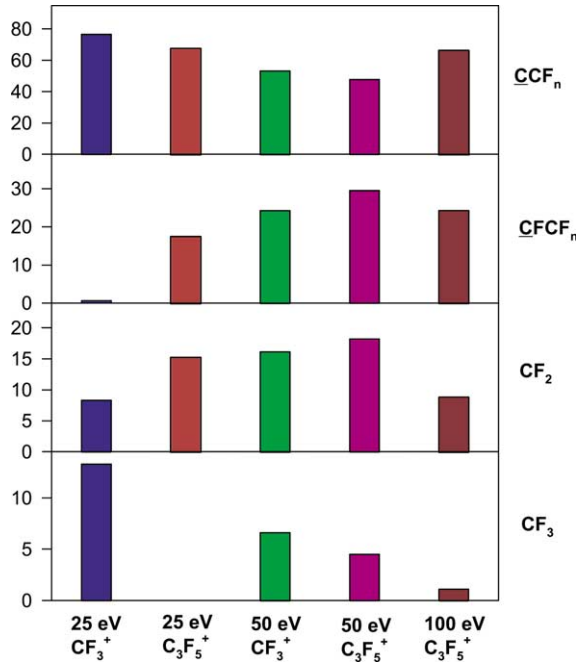

Fig. 5. Chemical composition of polystyrene thin films modified by 25–100 eV CF_3^+ and $C_3F_5^+$ ion beams, prepared with ion doses equivalent to 1.5×10^{16} F atoms/cm^2. The percentages of each fluorocarbon component are normalized by removal of the non-fluorinated component. These fluorocarbon films are several nm thick and 30–60% fluorine, with the remaining composition carbon. Figure adapted from Ref. [75].

leads to different polystyrene film chemistry, when compared at either similar total ion energy or energy/atom. These ions form a distribution of different fluorocarbon functional groups in amounts dependent upon the incident ion energy, structure, and fluence (Fig. 5). Both ions deposit mostly intact upon the surface at 25 eV, with $C_3F_5^+$ maintaining a structure similar to the proposed $CF_2{=}CFCF_2^+$ gas phase structure [74,75]. However, both ions undergo some polymerization upon deposition. Fragmentation of the ions increases as the ion energies are increased to 50 eV. Both ions form covalent bonds with the polystyrene surface at all energies. Finally, organic film growth from hyperthermal ions is actually a balance between growth and etching processes [8].

Further information on hyperthermal $C_3F_5^+$ deposition is obtained by molecular dynamics simulations on the analogous hydrocarbon system, $C_3H_5^+$ on polystyrene. Fig. 6 shows the effect of changes in the ionic structure, in this case $C_3H_5^+$, on the results of impacts with polystyrene at 50 eV [74,75]. In addition to the ground state CH_2–C^+H–CH_2 structure, two excited states are considered, CH_3–$C^+{=}CH_2$ and CH_3–CH–C^+H. Panels (a)–(c) in Fig. 6 show representative dissociation products for these isomers in snapshots from the simulations while panel (d) summarizes some of the important dissociation products that remain on the surface as a function of isomer type. Significant differences are predicted, such as the enhanced production of methyl radicals for isomers that already contain CH_3 structures. The simulations reaffirm that the ground state isomer is the most stable and predict that the CH_3–$CH{=}C^+H$ isomer is the easiest to dissociate on impact.

2.1.4. Organic cluster ion deposition

The deposition of carbon or hydrocarbon clusters is used to grow several types of films from polymeric to diamond-like carbon. Such films could be used as protective, lubricating coatings for computer hard disks, coatings for medical implants, or as dielectrics. As in the case of metal cluster deposition, the incident energy plays a crucial role in determining the structure and properties of the film. For example, when carbon cluster beams are deposited on metallic and polymeric surfaces at low velocities, nanostructured films form because the carbon clusters tend to retain their structure [76]. These films are found to have good adhesion to the substrate and may be used in electrochemical applications because of their stability and high surface area. In contrast, when carbon clusters ranging from tens to hundreds of atoms are deposited at thermal energies, similar nanostructured diamond-like films form that are only metastable with low adhesion to the substrate [77].

Atomistic simulations are used to study the chemistry that occurs within the cluster following organic cluster–surface impacts [78]. For instance, simulations describe the deposition of pure carbon clusters ranging in size from a few tens of atoms to a few hundreds of atoms, where the larger clusters are fullerenes. The clusters are deposited with energies of 0.1–1 eV/atom. The simulations reveal

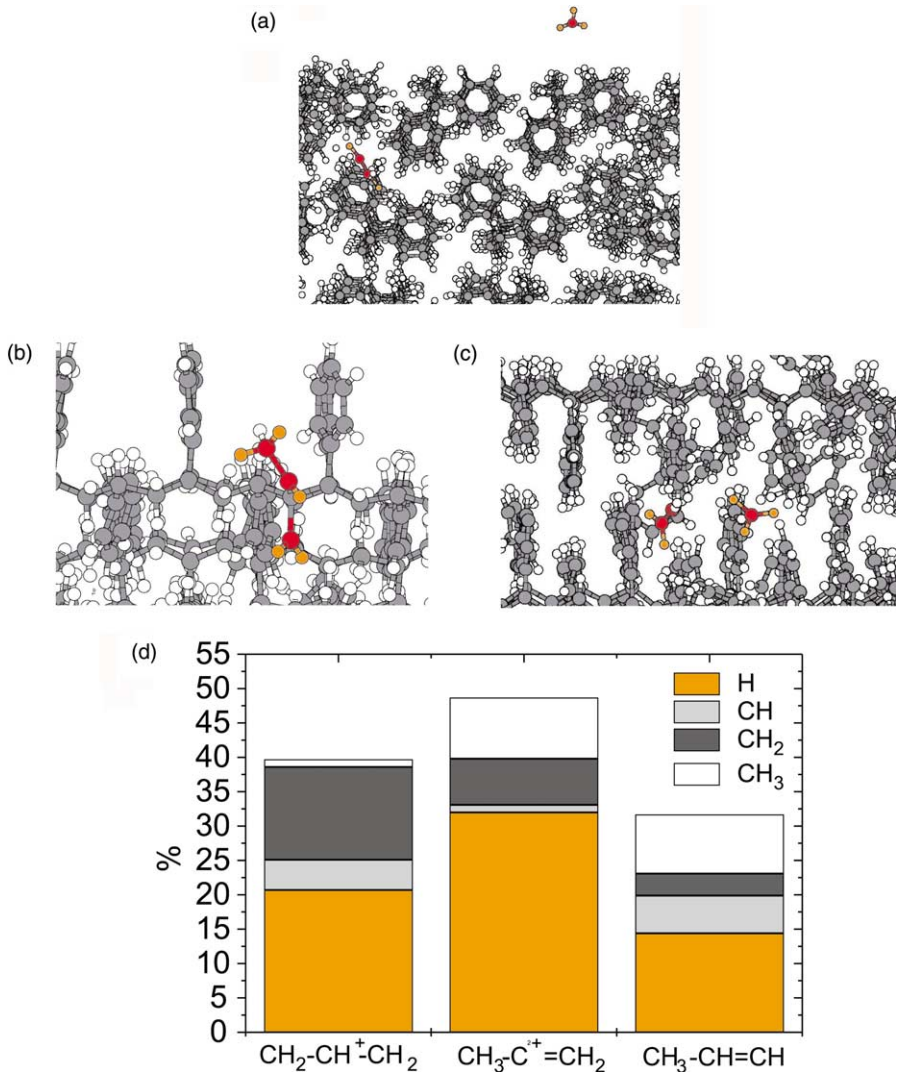

Fig. 6. The top three panels show snapshots from molecular dynamics simulations of three isomers of $C_3H_5^+$ deposited on polystyrene at incident energies of 50 eV. The bottom panel shows a statistical representation of some of the results. Panel (a) is a representative snapshot from the deposition of CH_3–CH–C^+H, panel (b) is a representative snapshot from the deposition of CH_2–C^+H–CH_2, and panel (c) is a representative snapshot from the deposition of CH_3–C^+–CH_2. Note how the ion fragments change with changes in the isomer structure. Panel (d) shows the percentage of the indicated products that remain bonded to or embedded in the polystyrene surface after deposition has fragmented the original ion. The results in panel (d) are averaged over 40 trajectories for each isomer to provide a statistical representation of possible outcomes. Figures adapted from Refs. [74,75].

that cluster size distribution plays a crucial role [79]. Films are homogeneous, graphitic, and relatively high density when grown with a bimodal distribution of cluster sizes and a larger fraction of small clusters compared to large clusters. Films are more porous and lower density with a random inhomogeneous, graphitic structure when a bimodal distribution is used with more large clusters than small clusters. Films become more dense and uniform as the clusters' energy increases—in agreement with experimental results—when a unimodal distribution of clusters is used.

Organic molecular clusters may also be deposited at energies of 5–80 eV/molecule. In this case collisions among the cluster molecules on impact play an important role in promoting addition chemistry and adhesion to the surface [80]. Consequently, the resulting films are polymeric rather than graphitic or diamond like. Clusters of more reactive molecules, such as ethylene, are predicted to form thin films at lower incident energies than clusters of less reactive molecules such as ethane [80]. Smaller clusters of a few tens of atoms form thin films more efficiently than large clusters of several hundred atoms which scatter most of their products away from the surface [81]. This result contrasts directly to what is predicted for metal clusters deposited on metal substrates. Finally, nucleation of the thin film depends on the reactivity of the surface [82], which can be influenced by the presence of a growing film [82,83].

2.2. Doping

Ion–surface collisions are intimately involved in several steps of the microelectronics manufacturing processes [84]. One crucial process is the doping of silicon wafers to create various features in complementary metal-oxide-semiconductor (CMOS) transistors [21]. Boron (B^+), phosphorous (P^+), and arsenic (As^+) are implanted into silicon at kinetic energies ranging from 5 keV to 1 MeV and doses ranging from 10^{11} to 10^{15} ions/cm^2. The dopant ion, its kinetic energy, and dose are selected depending upon the specific feature desired in the microelectronic device.

The need to shrink the dimensions of integrated circuits is progressing rapidly. The gate length of a CMOS transistor constructed on a silicon-based integrated circuit, 2 μm in 1975 and 0.35 μm in 1997, is now targeted to drop below 100 nm within the next few years [21]. Successful construction of these sub-100 nm CMOS transistors requires that B-doped regions be confined to similarly sized volumes of the Si substrate.

2.2.1. B doping of Si with low energy B^+

The keV to MeV energies of B^+ ion beams commonly used to dope Si substrates are expected to be too high to achieve sub-100 nm features. For example, 60 keV B^+ implantation in Si leads to a significant B concentration ranging from ~40 to ~260 nm below the surface [21]. Furthermore, the required annealing of the Si substrate subsequently leads to diffusion of the implanted B atoms which broadens this distribution out to an ~400 nm depth. When the B^+ initially impacts the surface, it creates a damage region known as a collision cascade, which is due to the secondary collisions of substrate atoms. This collision cascade region is composed of many Frenkel pairs, where a single Frenkel pair is defined as an interstitial atom (a Si atom that resides between the atoms in the regular Si crystalline lattice) and a vacancy (the space remaining in the lattice when that Si atom is removed). While many of these Frenkel pairs recombine upon annealing, defective regions remain that lead to damage-enhanced diffusion of the implanted B atoms. The ion implantation, thermal annealing, and defect production can be quite accurately predicted by Monte Carlo simulations.

The penetration depth of the ion into the Si substrate and the substrate defects are both roughly proportional to the ion energy: higher ion energies lead to deeper B penetration and greater numbers of substrate defects. Therefore, lower B^+ ion implantation energies reduce the spatial extent of the final B dopant profile and allow production of shallower CMOS transistor gates [21,85–87]. For example, a 2 keV B^+ ion implantation followed by annealing produces B-doped regions that are only 200 nm deep. B^+ ion implantation energies can be reduced again to 100–1000 eV, further narrowing the preannealing depth profile to below 100 nm. However, damage-enhanced diffusion that occurs when the substrate is subsequently annealed becomes the limiting factor in the final B depth distributions for <1 keV ions. Various annealing and preamorphization strategies have been considered to overcome the problem of damage-enhanced diffusion during annealing.

2.2.2. B doping of Si with low energy $B_{10}H_{14}^+$

Another method for producing ultrashallow junctions in Si is B doping with $B_{10}H_{14}^+$ [56,88]. One advantage of using $B_{10}H_{14}^+$ for B doping is the polyatomic-surface collision dynamics reduce the

implantation depth of the B individual atoms into the Si substrate. Although coulombic repulsion between ions becomes significant and begins to limit beam current at lower ion energies [21], the 10 B atoms per charge for a beam of $B_{10}H_{14}^{+}$ allows an order of magnitude greater flux of B atoms compared with a B^{+} at similar ion energy and current. Furthermore, the energy per atom for $B_{10}H_{14}^{+}$ is only 9% of that for B^{+} at similar absolute ion energy.

Molecular dynamics simulations on the impact of 4 keV $B_{10}H_{14}^{+}$ ions with Si [89] reveal that 90% of the preannealed, implanted B lies within 5 nm of the surface, although 10% of the B atoms are channeled to depths > 9 nm. The interstitial atoms and vacancies induced by 4 keV $B_{10}H_{14}^{+}$ ion impact are confined to the uppermost 5 nm of the surface. Fig. 7 displays the outcome for the impact of a single 4 keV $B_{10}H_{14}^{+}$ at the Si surface. Panel (a) of Fig. 7 displays the slight swelling and crater induced by the $B_{10}H_{14}^{+}$ impact. The same collision event at a 11.5 nm square Si crystal is shown from a different perspective in panel (b) to display the spatial distribution of the B atoms (orange balls), H atoms from $B_{10}H_{14}^{+}$ (green balls), and displaced surface Si atoms (purple balls). Panel (c) of Fig. 7 displays the same perspective as in panel (b), but displays only the interstitial Si atoms (purple balls). These results reveal that 4 keV $B_{10}H_{14}^{+}$ implantation in Si induces very shallow preannealed B doping and defect distributions. Experiments confirm the basic findings of the simulations [56,88,90], but other factors must be considered for commercial implementation [90].

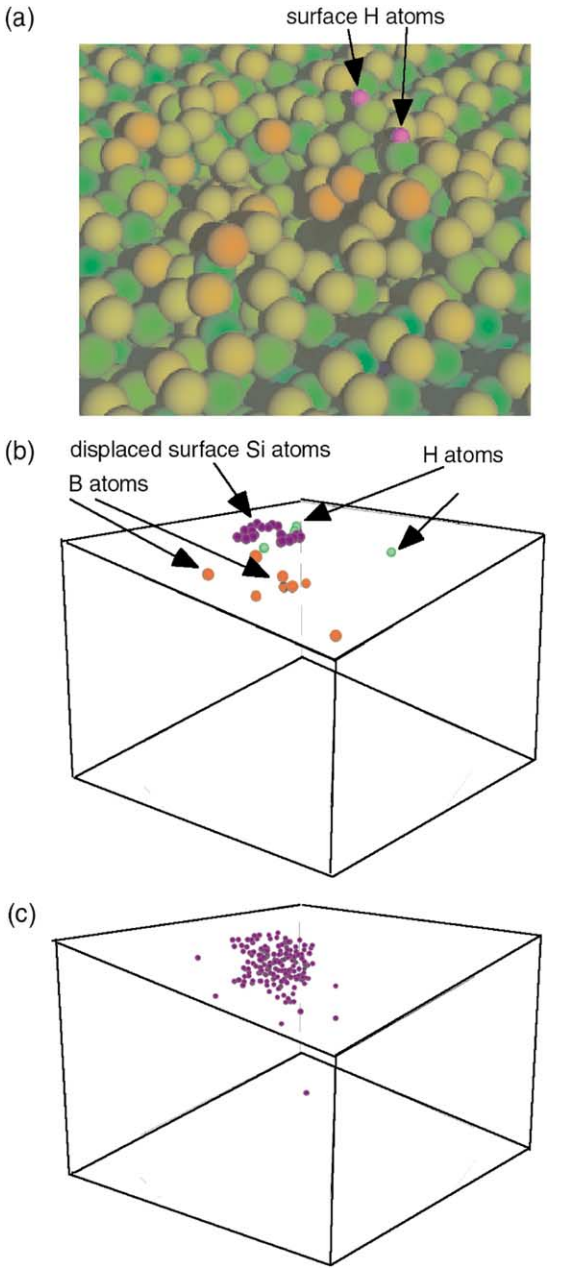

Fig. 7. Panel (a) shows the damage of a Si(1 0 0) crystal after impact of 4 keV $B_{10}H_{14}^{+}$. Note the surface swelling adjacent to a small crater. Panel (b) shows the crystal drawn from a different perspective where only the Si adatoms (purple balls) and the implanted atoms are shown (orange balls for B and green balls for H). Panel (c) displays the distribution of the interstitial Si atoms (purple balls). In panels (b) and (c), the crystal surface is 11.5 nm square. Figure used by permission of the American Institute of Physics [89].

2.3. Etching and lithography

2.3.1. Etching and growth of SiO on Si

Etching and lithography are two other processes in which ion–surface modification plays a central role [21–23,91]. The controlled growth of silicon oxide thin films from oxygen plasmas or ion beams is a method available for microelectronics manufacturing [5,84]. This thin-film growth process is balanced between deposition and etching processes. Fundamental reaction mechanisms inherent in these processes can be explored with a monoenergetic ion beam under ultrahigh vacuum

conditions. A Si(1 0 0) surface, exposed to 40–200 eV O^+ ions, develops a thin oxide film ~4 nm thick [92]. Further oxidation of the surface is balanced by erosion of the oxide layer during reactive O^+ ion bombardment. For example, 70 eV O^+ striking the SiO_x film produces various scattered ions: Si^+, SiO^+, O^-, and O_2^-. The product ion yields strongly increase with O^+ dose as the oxide film develops. Isotopic labeling experiments define the origin of each oxygen atom within the nascent O_2^- product [93]. An isotopically pure $Si^{16}O_x$ film is grown on Si(1 0 0) using a mass-filtered $^{16}O^+$ ion beam. Then the ion beam is switched to deliver only $^{18}O^+$ to the surface. The resulting scattered O_2^- products exhibit a mass of 34 amu exclusively, due to ^{18}O–$^{16}O^-$ [93]. It follows that O_2^- must be generated with an oxygen atom from the incident ion beam and an oxygen atom from the silicon oxide layer. The lack of signal at 32 and 36 amu demonstrated that O_2^- is not formed by sputtering of the oxide film or by recombination of two incident oxygen atoms, respectively. Measurements of the scattered ion angular and kinetic energy distributions (not shown) indicate that the peak of the scattered O_2^- flux lay near the specular angle. Furthermore, the mean kinetic energy of the O_2^- products increased linearly with incident O^+ kinetic energy. The correlation between incoming O^+ momentum and outgoing O_2^- momentum provides strong evidence for a direct abstraction mechanism [94]. This contrasts with the Si^+, SiO^+ and O^- product channels, where cascade sputtering accounts for the majority of the observed signal.

2.3.2. Repairing photomasks with focused ion beams

One commercial application for focused ion beams is the repair of photomasks. Photomasks are the templates used for transferring the patterns of microelectronic circuitry from a computer design file onto raw Si wafers via optical lithography [84]. The photomask is a glass plate with Cr features that are transferred onto the glass surface by an electron beam or laser writing process. Each photomask is inspected following production to reveal errors in the writing process. Two types of errors are typical: either extraneous Cr features appear where they do not belong or Cr features are missing where they should appear. These errors are corrected by use of a focused ion beam repair tool [95]. This instrument has a low energy Ga^+ beam that is focused to ~100 nm. It also has a secondary ion mass spectrometry imaging system that distinguishes Cr^+ sputtered from the Cr features by the incident Ga^+ ion beam from Si^+ sputtered from the glass. Extraneous Cr features are repaired by sputtering them away with the Ga^+ beam until the Cr^+ signal is no longer observed. Panel (a) in Fig. 8 displays a photomask with Cr features displayed as blue and glass features as

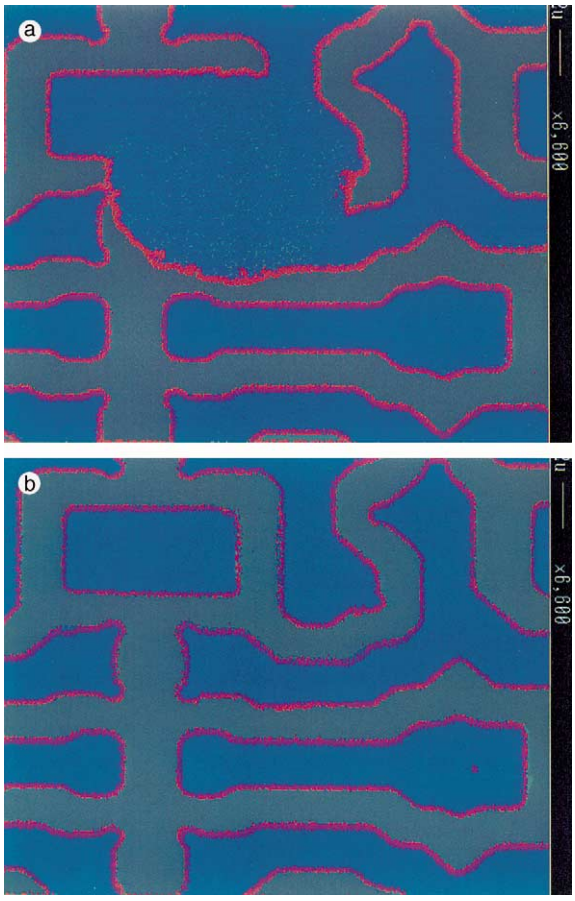

Fig. 8. Panel (a) shows a photomask with Cr features displayed as blue and glass features as either gray or pink when adjacent to Cr (bar at right = 2 μm length). A large blue feature corresponding to extraneous Cr dominates the upper center. Panel (b) shows the same photomask following repair with the Ga^+ ion beam: the extraneous Cr feature is now missing and has been replaced with the correct Cr/glass pattern.

either gray or pink when adjacent to Cr (bar at right = 2 μm length). A large blue feature corresponding to extraneous Cr dominates the upper center of panel (a). Panel (b) in Fig. 8 displays the photomask following repair with the Ga^+ ion beam: the extraneous Cr feature is missing and has been replaced with the correct Cr/glass pattern. Missing Cr features also can be repaired by Ga^+ ion beam stimulated deposition of graphitic carbon onto the glass surface. Graphite carbon is formed by decomposition of an adsorbed organic compound by the energetic Ga^+ ions. The organic compound can be pyrene, styrene, indene, or other aromatic hydrocarbon that is introduced as a vapor into the system [96].

2.3.3. Patterning self-assembled monolayers and polymers

Ion beam etching also can be used to pattern organic materials and polymers. 50–140 eV Ar^+ ion beams may be used to pattern organosilane self-assembled monolayers by simply masking a portion of the beam from the monolayer [97]. The ion beam patterns are then transformed into >100 nm thick Ni features by a wet chemical process known as electroless metallization. Poly(methyl methacrylate) and other polymeric photoresists also can be etched by a ~100 keV broad beam of H^+, H_2^+, or He^+ ions projected through a stencil mask that blocks portions of the beam [22,23]. This technology is the basis for ion projection lithography, which is being considered for sub-100 nm lithography to produce the next generation of microelectronics devices. Alternatively, 300 nm line widths may be created on organosilane self-assembled monolayers by focused beams of 50–280 keV Ga^+, Si^{2+}, Au^+, and Au^{2+} followed by electroless metallization [97]. These line widths readily can be narrowed to <50 nm by better ion beam focusing [21]. Photoresist polymers also can be etched by focused ion beams [98].

2.4. Materials Toughening

2.4.1. Toughening polymers with keV–MeV atomic ion beams

Ion implantation of polymeric materials can produce a hard and wear-resistant surface while maintaining the bulk properties of the polymers [99]. Such changes could allow for polymers to be used in, for example, manufacturing applications where mechanical degradation is currently a problem. These improved properties result from cross-linking at the polymer surface caused by localized structural damage from the ions. Increasing the incident energy increases the penetration depth of the ions but does not increase the amount of cross-linking. For ion energies of several hundreds of keV to several MeV, the modification depth is only a few microns, with the exact depth decreasing as the mass of the incident ion increases. However, ions with higher masses are more efficient at inducing the surface cross-linking than lighter ions. To get a good balance between depth and efficiency of cross-linking, multiple ions (e.g., He^+ and Ar^+ at 1 MeV) can be used [100, 101].

Ion implantation has been used successfully to modify several polymers such as polycarbonate, polyimide, polystyrene, and polyetheretherketone. Ion implantation can lead to increases in hardness of about two orders of magnitude and reduction of friction coefficients by about one order of magnitude. Polytetrafluoroethylene and certain other polymers do not respond well to ion bombardment, however, and simply degrade. It is thought [102] that when the incident ions transfer their energy to the surface through ionization or electronic excitation of the substrate atoms, cross-linking results, while direct nuclear collisions that scatter the ions result in surface degradation. Classical molecular dynamics simulations of ion implantation on polyethylene [103,104] predict, however, significant cross-linking near the surface without including electronic effects. They also predict that the ratio of broken C–H to C–C bonds decreases with the increasing mass of the ions and that the total number of bonds broken depends linearly on the incident energy in agreement with experimental observations.

2.4.2. Toughening steel with keV–MeV atomic ion beams

The implantation of N, C, O, Hf, Er, Cr, Ti, and Y ions into steel significantly improves the hardness, toughness and wear properties of these

materials [105–111]. In addition, the friction coefficients are decreased [112,113]. These findings have important implications for steel tools for which considerable cost savings could be achieved if the lifetimes of active use of the tools could be extended. The ions are generally implanted at low to medium energies, leading to considerable changes in the structure and microstructure of the surface and near-surface regions of the alloy. The mechanisms by which these various ions modify the mechanical properties of the material are not well understood and appear to depend on the type of ion implanted. For example, there is evidence that carbon implantation leads to the formation of amorphous areas with fine metal carbide grains and graphitic phases that could act as lubricating layers [112,113]. In the case of nitrogen implantation, hard metal nitride formation is thought to be responsible for the increased hardness of steel, while oxygen ion bombardment leads to the formation of oxide layers in the near-surface region of the steel [114]. Studies [114–118] have also found that implanting a metal ion and an oxygen ion either at the same time or sequentially leads to even greater improvement in the mechanical properties of the steel. When one considers the implications of this research just on manufacturing and the lack of fundamental understanding of the mechanisms behind these results, it is clear that this area deserves further study at both the fundamental and applied level.

3. The future

The examples developed in the previous section show that the growth and modification of materials through ion–surface processing can be used to create a wide range of materials for a variety of applications. Nevertheless, the mechanisms by which many of these processes occur remain undetermined. This is especially true for materials that are themselves inherently complex. For example, it is difficult to determine fundamental mechanisms for ion modification of steel, which contains numerous components and whose microstructure and properties can vary widely with changes in processing conditions. It is expected that an improved understanding of these mechanisms should lead to important improvements in manufacturing that are crucial for the processing of the next generation of tools and devices. An indication of research areas for which ion–surface modification promises considerable scientific and technological advances in the new millennium is provided below.

3.1. Formation of nanostructures

Nanometer-scale structured films and materials (nanostructures) are an increasingly active area of research because they promise unique mechanical, electronic, and chemical properties. One area for future advances is increased process control for the doping of electronic materials as the dimensions of electronic devices continue to shrink. A promising new direction is the creation of buried interfaces by doping selective regions of microelectronic circuits with medium energy ion beams. In addition, metallic superlattice structures can exhibit giant magnetoresistance provided they are grown with smooth, defect-free interface structures. Improvements in ion–surface processing could result in the manufacture of superlattice structures with more layers that will have the necessary properties to be used as sensors, disk drives, or memory elements.

One area where nanoscale science has already begun to interact with ion–surface modification is the energetic surface collisions of C_{60}^{+} and other fullerene ions. Thermal deposition of buckyball fullerenes (C_{60}) leads the formation of nanostructured thin films where the components of the film retain the electronic structure of the deposited buckyballs [77,119]. Simulations of 0.15 keV C_{60} deposition predict both reactive and elastic collisions [120]. Experiments at similar energies [121] find that 0.15 keV impacts depend greatly on the nature of the substrate being impacted. At 0.5 keV, graphite targets will scatter back some of the incident buckyballs, while metal substrates flatten and dissociate them. At $\sim$1 keV, smooth, amorphous, diamond-like, hydrogen-free films are produced that contain graphitic crystallites embedded within the amorphous lattice [121]. Atomistic simulations at $\sim$1 keV show the buckyballs fall apart and the atoms then agglomerate within the

surface to form carbon nanostructures [122]. At energies of several keV, simulations predict that a hot zone develops in the area of impact that propagates away in waves [123]. This leads to the formation of protrusions and hillocks that have been experimentally observed [124].

Fullerene–surface collisions are but one means of forming nanostructures by the transfer of intact nanometer-sized species to surfaces. Formation of nanostructures also can be accomplished with metal cluster ion deposition (see Section 2). These methods are being explored to make novel cluster catalyst materials that are stabilized against sintering. Biomolecular ions—formed by methods developed for biomolecular mass spectrometry [125]—can also be collided with surfaces to form nanostructures. For example, 150 keV lysozyme ion impacts create well-defined nm sized defects in graphite [126]. In fact, the shapes of these surface defects are used to determine the gas phase structure of the lysozyme ion. The size of biomolecular ions can range from <0.5 to >10 nm, depending upon their mass and structure: deposition of these ions opens the possibility of nanostructured surfaces with similar (albeit random) dimensionality. More subtle effects might occur at yet lower energies. For example, ion scattering studies of 200–700 amu peptide ions found a strong dependence in ion–surface energy transfer with peptide mass [127]. These unusual energy transfer effects could translate into new phenomena in biomolecular ion–surface modification.

The nanostructure of ion-induced substrate features also is affected by the ion-induced collision cascades that extend into the 10s nm range as the ion energy approaches 10 keV. MeV ion–surface bombardment can transfer a large amount of energy to the substrate, albeit via electronic excitations. These electronic excitations cause collision cascades within the substrate and can lead to the formation of unusual defects and nanostructures with unique properties (e.g., damage tracks extended deep into a substrate) (for example, see Ref. [128] and other articles in that issue).

Simple sputtering of surfaces with low energy atomic ions can lead to regular or irregular nanostructures. Cones can form on surfaces by removal of material around impurities that sputter inefficiently [7]. Tuning the incident ion angle and surface temperature can cause nm-sized regular ripples on a surface formed by competition between erosion and surface atom diffusion [129]. Hyperthermal ion sputtering of graphite followed by reactive etching with oxygen gas forms well-defined nm-scale etch pits [130]. Researchers are increasingly likely to produce unique nanostructures by various combinations of low energy ion sputtering, deposition of sputtered atoms, annealing, and gas–surface reactions. Slow multiply charged ions also can be used to produce nanostructures due to their unique charge transfer-induced sputtering mechanism [131].

Hyperthermal polyatomic ions can also be used to generate nanostructures at interfaces. Fig. 9 is an image from an atomic force microscope (in tapping mode) of a fluorocarbon film grown on a polystyrene surface by 100 and 50 eV $C_3F_5^+$ (see Fig. 5 for chemical analysis of this same surface). Both dimensions of these features vary considerably with ion energy. The polyatomic ion energy, fluence, and identity thereby constitute direct means of controlling the nanostructure on an interface. Nanostructuring of polystyrene is also observed for low energy atomic ion bombardment [132].

Yet another means of nanostructuring interface regions is via focused ion beams (see Section 2). Focused ion beams with beamwidths as narrow as 20 nm are now available and can be employed for lithography via ion exposure of a resist, ion milling, gas-assisted etching, and ion assisted deposition of material [133]. Three-dimensional nanoscale patterning is feasible with focused ion beams [134]. Focused ion beams or ion projection lithography also can be combined with microcontact printing techniques to nanopattern even curved surfaces [135].

3.2. Combinatorial searching of new materials

Combinatorial materials science is rapidly becoming the dominant means by which new materials with favorable properties are discovered [136]. The method involves the production of a two-dimensional array of material samples (library)

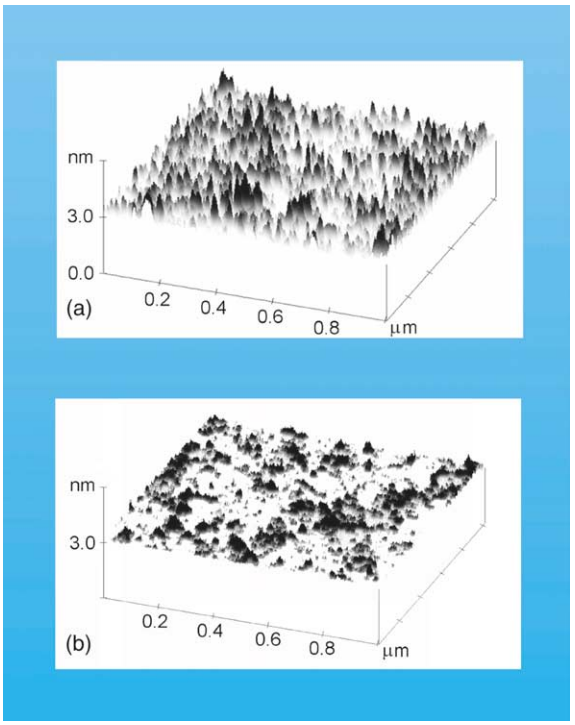

Fig. 9. Panel (a) shows the atomic force microscope image of fluorocarbon film grown on a polystyrene surface by 100 eV $C_3F_5^+$ ions. Panel (b) is the same except the film is formed by 50 eV ions. (see Fig. 5 for chemical analysis of this same surface). Differently shaped features with size ranging from 1.5 to 3.0 nm are observed for both ion-modified surfaces. The roughnesses of the 50 and 100 eV $C_3F_5^+$ ion-modified polystyrene surfaces are 1.8 ± 0.2 and 7.4 ± 0.6 Å (RMS), respectively, indicating that the higher ion energy leads to a rougher surface. By contrast, the roughness of the unmodified polystyrene surface is 1.0 ± 0.2 Å.

with each sample produced under slightly different processing conditions. These libraries are screened for desirable physical properties, then the data used to further refine the processing conditions or the optimal sample selected for use. The entire process is typically highly automated to permit the rapid screening of large numbers of libraries. Libraries also can be produced as a continuous film with smoothly varying processing conditions [137]. Ion beam processing is ideal for combinatorial searching of new materials since it is simple to vary the ion energy, fluence, or ion identity in an automated fashion [151].

3.3. Biointerfaces

Biointerfaces are widely considered one of the important frontiers in surface and interface science (see the article by Matthew Tirrell in this volume). Several ion–surface modification strategies are being actively employed to create surfaces with tailored biological activity by controlling their chemistry, morphology, or mechanical properties. Ion implantation improves corrosion resistance or reduces wear in implanted metal devices [138]. Low energy Mg^+ implantation into alumina improves the growth of bone cells on the alumina surface [139]. Low energy Ar^+ ion bombardment of a polysiloxane polymer surface improves fibroblast cell growth on this polymer [140]. Focused ion beams are used to create nm-scale defects with controlled protein adsorption properties [141]. A significant advantage from a regulatory standpoint is the extremely small amounts of material deposited from the ion beam are often considered unlikely to induce toxic or other unfavorable responses when in contact with human tissue. These facts all indicate that ion–surface modification will play an increasingly important role in the production of biointerfaces.

The deposition of intact biological and synthetic polymers on surfaces shows promise for creating new biointerfaces [125,142–147]. Even large DNA ions have been soft-landed intact on surfaces [144]. These techniques are now being explored for the creation of arrays for use in combinatorial chemistry or chemical sensors. Intense beams of large biomolecular ions can be readily produced, although depending upon experimental conditions the ions so produced can be neat, clustered to solvent molecules, or dissolved in micron-sized solvent droplets. Furthermore, the characteristics of films deposited by these methods have been explored only briefly. For example, these experiments have not applied surface analysis methodologies beyond scanning probe microscopy and mass spectral analysis of the deposited species by redesorption/ionization. Nevertheless, these techniques open up an entirely new class of molecular and biomolecular species for use in ion–surface modification of biointerfaces.

3.4. Isotopically pure materials

Mass-selected ion beams are inherently composed of a single isotope and therefore can be employed to create isotopically pure materials interfaces or dopants in materials. Controlling the isotopic distribution of a materials interface promises to affect at least its thermal conductivity and refractive index. Isotopically pure films of ^{28}Si on Si(1 0 0) and ^{107}Ag on Ni(1 0 0) can be grown from the corresponding hyperthermal atomic ions [148,149]. Technical limitations such as low vacuum conditions can complicate the production of isotopically pure materials. Nevertheless, once these experimental difficulties are overcome, a wide range of isotopically pure materials interfaces can begin to be explored in depth.

3.5. Challenges to manufacturing with ion–surface processing

A major challenge for the expansion of ion–surface processing into high volume manufacturing is the relatively high cost associated with these methods. Decreasing the processing cost so that it is the same order of magnitude as paint application, for example, would dramatically increase its use in a variety of industries where it is currently cost prohibitive, such as the automotive industry. However, ion–surface processing possesses a considerable environmental advantage over wet chemical methods in that the former employs no solvents and wastes little reagent. This savings in chemical purchase and disposal costs can sometimes compensate for the added capital costs of ion-modification equipment.

Other details of the manufacturing process also dictate whether ion–surface processing becomes more widely utilized. These include the ability to produce ion beams of sufficient high ion current to reduce processing times and the determination whether mass selection of the ions is always required for a given process. One possible strategy is to use mass-selected ion beams to prototype new materials, then actually manufacture them in bulk by plasma, magnetron sputtering, or other methods already adapted to the industrial scale. Finally, ion–surface modification must still compete with other, often equally powerful technologies. For example, sub-100 nm ion projection lithography is viable, but it must still compete with electron, vacuum ultraviolet, and X-ray lithography for a place in the large-scale production of microelectronic circuits.

Simulations are increasingly being applied to engineering processes of technological importance. In the near future these models may be used in production settings to adjust manufacturing conditions, especially for processes that are somewhat simple, such as sputtering and doping. Atomistic simulations are usually applied to systems that have been simplified somewhat from actual manufacturing conditions. However, as computing power continues to increase and the devices being manufactured continue to decrease in size, it is increasingly useful to apply atomistic approaches to product design.

In conclusion, ion–surface processing promises a rich yield of new, rationally designed materials for technological applications in the new millennium. It also promises to yield many exciting advances in fundamental knowledge regarding the growth of new materials by a combination of experimental and computational approaches.

Acknowledgements

The authors would like to thank the many people who contributed in various ways to the production of this article. Dennis Jacobs and his students at the University of Notre Dame provided Fig. 1. Michael Moseler of the Georgia Institute of Technology and Hellmut Haberland of the Freiburg Materials Research Center provided Fig. 4. Roger Smith of Loughborough University and Roger Webb of University of Surrey provided Fig. 7. Steve Ruatta of Photronics provided Fig. 8. Gerry Zajac of BP Amoco provided scientific assistance and access to the atomic force microscope used to collect the data for Fig. 9. Wayne Rabalais of the University of Houston and Yip-Wah Chung of Northwestern University provided reprints, preprints, and instructive information on isotopically pure and carbon nitride films, respectively. LH's graduate students Muthu Wijesundara and Erick

Fuoco of the University of Illinois at Chicago collected the data in Figs. 5 and 9. SBS's students and postdoctoral research associates Yuan Ji, and Boris Ni ran the molecular dynamics simulations presented in Fig. 6. Finally, the National Science Foundation and the Petroleum Research Fund provided funding for the authors' research efforts in ion–surface collisions (LH: NSF CHE-9986226; SBS: NSF CHE-9708049).

References

[1] J.E. Greene, T. Motooka, J.-E. Sundgren, D. Lubben, S. Gorbatkin, S.A. Barnett, The role of ion/surface interactions and photo-induced reactions during film growth from the vapor phase, Nucl. Instrum. Meth. Phys. Res. B 27 (1987) 226–242.

[2] J.J. Cuomo, S.M. Rossnagel, H.R. Kaufman (Eds.), Handbook of Ion Beam Processing Technology: Principles Deposition Film Modification and Synthesis, Noyes Publications, Park Ridge, 1989.

[3] S.R. Kasi, H. Kang, C.S. Sass, J.W. Rabalais, Inelastic processes in ion–surface collisions, Surf. Sci. Rep. 10 (1989) 1–105.

[4] E. Taglauer, Surface cleaning using sputtering, Appl. Phys. A 51 (1990) 238–251.

[5] J.W. Rabalais (Ed.), Low Energy Ion–Surface Interactions, Wiley, Chichester, 1994.

[6] M. Nastasi, J.W. Mayer, J.K. Hirvonen, Ion–Solid Interactions: Fundamentals and Applications, Cambridge University Press, Cambridge, 1996.

[7] V.S. Smentkowski, Trends in sputtering, Prog. Surf. Sci 64 (2000) 1–58.

[8] W. Jacob, Surface reactions during growth and erosion of hydrocarbon films, Thin Solid Films 326 (1998) 1–42.

[9] A. Benninghoven, F.G. Rudenauer, H.W. Werner, Secondary Ion Mass Spectrometry: Basic Concepts, Instrumental Aspects, Applications and Trends, Wiley, New York, 1987.

[10] L. Hanley, O. Kornienko, E.T. Ada, E. Fuoco, J.L. Trevor, Surface mass spectrometry of molecular species, J. Mass Spectrom. 34 (1999) 705–723.

[11] J.F. Ziegler, J.P. Biersack, U. Littmark, The Stopping and Range of Ions in Solids, Pergamon Press, New York, 1985.

[12] X.-Y. Zhu, Surface photochemistry, Annu. Rev. Phys. Chem. 45 (1994) 113–144.

[13] E.T. Ada, L. Hanley, Comparing hyperthermal molecular and atomic ion sputtering of adsorbates: Xe^+ vs. SF_5^+ on NH_3/CO/Ni(1 1 1), Int. J. Mass Spectrom. Ion Process. 174 (1998) 231–244.

[14] W.D. Sproul, Multi-cathode unbalanced magnetron sputtering systems, Surf. Coat. Technol. 49 (1991) 284–289.

[15] W. Ensinger, Plasma immersion ion implantation for metallurgical and semiconductor research and development, Nucl. Instrum. Meth. Phys. Res. B 120 (1996) 270–281.

[16] D.J. Rej, H.A. Davis, J.C. Olson, G.E. Remnev, A.N. Zakoutaev, V.A. Ryzhkov, V.K. Struts, I.F. Isakov, V.A. Shulov, N.A. Nochevnaya, et al., Materials processing with intense pulsed ion beams, J. Vac. Sci. Technol. A 15 (1997) 1089–1097.

[17] S.M. Rossnagel, Directional and ionized physical vapor deposition for microelectronics applications, J. Vac. Sci. Technol. B 16 (1998) 2585–2608.

[18] W.R. Sobie, Ion beam technology for thin film applications, Vacuum and Thinfilm, April 1999 (pp. 36–39).

[19] P.J. Martin, A. Bendavid, H. Takikawa, Ionized plasma vapor deposition and filtered arc deposition: processes, properties, and applications, J. Vac. Sci. Technol. A 17 (1999) 2351–2359.

[20] M.E. Graham, Directions in PVD coatings, in: A. Kumar, Y.-W. Chung, J.J. Moore, J.E. Smugeresky (Eds.), Surface Engineering: Science and Technology I, The Minerals, Metals and Materials Society, 1999.

[21] E. Chanson, S.T. Picraux, J.M. Poate, J.O. Borland, M.I. Current, T. Diaz de la Rubia, D.J. Eaglesham, O.W. Holland, M.E. Law, C.W. Magee, et al., Ion beams in silicon processing and characterization, J. Appl. Phys. 81 (1997) 6513–6561.

[22] J. Melgailis, A.A. Mondelli, I.L. Berry, R. Mohondro, A review of ion projection lithography, J. Vac. Sci. Technol. B 16 (1998) 927–957.

[23] R. Kaesmaier, H. Loschner, G. Stengl, J.C. Wolfe, P. Ruchhoeft, Ion projection lithography: international development program, J. Vac. Sci. Technol. B 17 (1999) 3091–3097.

[24] B.J. Garrison, P.D.S. Kodali, D. Srivastava, Modeling of surface processes as exemplified by hydrocarbon reactions, Chem. Rev. 96 (1996) 1327–1341.

[25] S.M. Foiles, M.I. Baskes, M.S. Daw, Embedded-atom-method functions functions for the FCC metals Cu, Ag, Au, Ni, Pd, Pt, and their alloys, Phys. Rev. B 33 (1986) 7983.

[26] J. Tersoff, New empirical potential for the structural properties of silicon, Phys. Rev. Lett. 56 (1986) 632.

[27] D.W. Brenner, Empirical potential for hydrocarbons for use in simulating the chemical vapor deposition of diamond films, Phys. Rev. B 42 (1990) 9458–9471.

[28] M.P. Allen, D.J. Tildesley, Computer Simulation of Liquids, Oxford University Press, New York, 1987.

[29] R. Carr, M. Parrinello, Unified approach for molecular dynamics and density-functional theory, Phys. Rev. Lett. 55 (1985) 5311.

[30] C.S. Jayanthi, S.Y. Wu, J. Cocks, Z.L.X.N.S. Luo, M. Menon, G. Yang, Order-N method for a nonorthogonal tight-binding Hamiltonian, Phys. Rev. B 57 (1998) 3799.

[31] R.S. Averback, M. Ghaly, Fundamental aspects of defect production in solids, Nucl. Instrum. Meth. Phys. Res. B 127 (1997) 127.

[32] M.H. Shapiro, T.A. Tombrello, Simulation of core excitation during cluster impacts, Phys. Rev. Lett. 68 (1992) 1613.
[33] W. Eckstein, Computer Simulation of Ion–Solid Interactions, Springer, New York, 1991.
[34] J.P. Biersack, L. Haggmark, A Monte Carlo computer program for the transport of energetic ions in amorphous targets, Nucl. Instrum. Meth. Phys. Res. 174 (1980) 257.
[35] K.J. Boyd, D. Marton, J.W. Rabalais, S. Uhlmann, T. Frauenheim, Semiquantitative subplantation model for low energy ion interactions with surfaces. I. Noble gas ion–surface interactions, J. Vac. Sci. Technol. A 16 (1998) 444–454.
[36] K.J. Boyd, D. Marton, J.W. Rabalais, Y. Lifshitz, Semiquantitative subplantation model for low energy ion interactions with surfaces. II. Ion beam deposition of carbon and carbon nitride, J. Vac. Sci. Technol. A 16 (1998) 455–462.
[37] K.J. Boyd, D. Marton, J.W. Rabalais, S. Uhlmann, T. Frauenheim, Semiquantitative subplantation model for low energy ion interactions with surfaces. III. Ion beam homoepitaxy of Si, J. Vac. Sci. Technol. A 16 (1998) 463–471.
[38] W.D. Sproul, New routes in the preparation of mechanically hard films, Science 273 (1996) 889–892.
[39] A.Y. Liu, M.L. Cohen, Structural properties and electronic structure of low-compressibility materials: β-Si_3N_4 and hypothetical β-C_3N_4, Phys. Rev. B 41 (1990) 10727.
[40] D. Marton, K.J. Boyd, A.H. Al-Bayati, S.S. Todorov, J.W. Rabalais, Carbon nitride deposited using energetic species: a two-phase system, Phys. Rev. Lett. 73 (1994) 118.
[41] K.J. Boyd, D. Marton, S.S. Todorov, A.H. Al-Bayati, J. Kulik, R.A. Zuhr, J.W. Rabalais, Formation of C–N thin films by ion beam deposition, J. Vac. Sci. Technol. A 13 (1995) 2110.
[42] C. Ronning, H. Feldermann, R. Merk, H. Hofsass, P. Reinke, J.-U. Thiele, Carbon nitride deposited using energetic species: a review on XPS studies, Phys. Rev. B 58 (1998) 2207–2215.
[43] I. Gouzman, R. Brener, A. Hoffman, Electron spectroscopic study of C–N bond formation by low-energy nitrogen ion implantation of graphite and diamond surfaces, J. Vac. Sci. Technol. A 17 (1999) 411.
[44] N. Tsubouchi, B. Enders, A. Chayahara, A. Kinomura, Optical properties of carbon and carbon nitride films prepared by mass-separated energetic negative carbon and carbon nitrogen ions, J. Vac. Sci. Technol. A 17 (1999) 2384.
[45] B.Z. Zhou, Y.-W. Chung, Recent advances in the synthesis and properties of amorphous and crystalline carbon nitride, J. Chin. Inst. Eng. 21 (1998) 691–700.
[46] W.-C. Chan, B. Zhou, Y.-W. Chung, C.S. Lee, S.T. Lee, Synthesis, composition, surface roughness and mechanical properties of thin nitrogenated carbon films, J. Vac. Sci. Technol. A 16 (1998) 1907–1911.
[47] M.L. Wu, M.U. Guruz, V.P. Dravid, Y.-W. Chung, S. Anders, F.L. Freire Jr., G. Mariotto, Formation of carbon nitride with sp^3-bonded carbon in CN_x/ZrN superlattice coatings, Appl. Phys. Lett. 76 (2000) 2692–2694.
[48] X.W. Zhou, H.N.G. Wadley, Atomistic simulations of the vapor deposition of Ni/Cu/Ni multilayers: the effects of adatom incident energy, J. Appl. Phys. 84 (1998) 2301.
[49] J. Jacobsen, B.H. Cooper, J.P. Sethna, Simulations of energetic beam deposition: from picoseconds to seconds, Phys. Rev. B 58 (1998) 15847.
[50] S. van Dijken, L.C. Jorritsma, B. Poelsema, Grazing-incidence metal deposition: pattern formation and slope selection, Phys. Rev. B 61 (2000) 14047.
[51] C.F. Abrams, D.B. Graves, Cu sputtering and deposition by off-normal, near-threshold Cu^+ bombardment: molecular dynamics simulations, J. Appl. Phys. 86 (1999) 2263.
[52] M. Ghaly, R.S. Averback, The formation of vacancy-type defect clusters by ion bombardment: a problem revisited with molecular dynamics, J. Phys. Chem. Solids 55 (1994) 945–953.
[53] K. Nordlund, M. Ghaly, R.S. Averback, M. Caturla, T. Diaz de la Rubia, J. Tarus, Defect production in collision cascades in elemental semiconductors and fcc metals, Phys. Rev. B 57 (1998) 7556.
[54] K. Nordlund, R.S. Averback, Point defect movement and annealing in collision cascades, Phys. Rev. B 56 (1997) 2321.
[55] N. Toyoda, H. Kitani, J. Matsuo, I. Yamada, Reactive sputtering by SF_6 cluster ion beams, Nucl. Instrum. Meth. Phys. Res. B 121 (1997) 484–488.
[56] D. Takeuchi, N. Shimada, J. Matsuo, I. Yamada, Shallow junction formation by polyatomic cluster ion implantation, Nucl. Instrum. Meth. Phys. Res. B 121 (1997) 345–348.
[57] W.L. Brown, M.F. Jarrold, R.L. McEachern, M. Sosnowski, G. Takaoka, H. Usui, I. Yamada, Ion cluster beam deposition of thin films, Nucl. Instrum. Meth. Phys. Res. B 59/60 (1991) 182.
[58] H. Haberland, M. Karrais, M. Mall, Y. Thurner, Thin films from energetic cluster impact: a feasibility study, J. Vac. Sci. Technol. A 10 (1992) 3266.
[59] H. Haberland, M. Mall, M. Moseler, Y. Qiang, T. Reiners, Y. Thurner, Filling of micron-sized contact holes with copper by energetic cluster impact, J. Vac. Sci. Technol. A 12 (1994) 2925.
[60] H. Haberland, Z. Insepov, M. Moseler, Molecular-dynamics simulation of thin-film growth by energetic cluster impact, Phys. Rev. B 51 (1995) 11061.
[61] H. Haberland, Z. Insepov, M. Karrais, M. Mall, M. Moseler, Y. Thurner, Thin films from energetic cluster impact: experiment and molecular dynamics simulations, Nucl. Instrum. Meth. Phys. Res. B 80/81 (1993) 1320.
[62] M. Moseler, O. Rattunde, J. Nordiek, H. Haberland, On the origin of surface smoothing by energetic cluster impact: molecular dynamics simulation and mesoscopic

modeling, Nucl. Instrum. Meth. Phys. Res. B 164/165 (2000) 522.
[63] M. Moseler, J. Nordiek, O. Rattunde, H. Haberland, Simple models for film growth by energetic cluster impact, Radiat. Eff. 142 (1997) 38.
[64] W. Bouwen, E. Kunnen, K. Temst, P. Thoen, M.J. Van Bael, F. Vanhoutte, H. Weidele, P. Lievens, R.E. Silverans, Characterization of granular Ag films grown by low-energy cluster beam deposition, Thin Solid Films 354 (1999) 87.
[65] H. Hsieh, R.S. Averback, Molecular-dynamics investigations of cluster-beam deposition, Phys. Rev. B 42 (1990) 5365.
[66] H. Hsieh, R.S. Averback, H. Sellers, C.P. Flynn, Molecular-dynamics simulations of collisions between energetic clusters of atoms and metal substrates, Phys. Rev. B 45 (1992) 4417.
[67] R.S. Averback, M. Ghaly, H. Zhu, Cluster–solid interactions: a molecular dynamics investigation, Radiat. Eff. Defects Solids 130–131 (1994) 211.
[68] G. Vandoni, C. Felix, C. Massobrio, Molecular-dynamics study of collision, implantation and fragmentation of Ag7 on Pd(100), Phys. Rev. B 54 (1996) 1553.
[69] W.M. Lau, R.W.M. Kwok, Engineering surface reactions with polyatomic ions, Int. J. Mass Spectrom. Ion Process. 174 (1998) 245–252.
[70] E.T. Ada, O. Kornienko, L. Hanley, Chemical modification of polystyrene surfaces by low-energy polyatomic ion beams, J. Phys. Chem. B 102 (1998) 3959–3966.
[71] S.A. Miller, H. Luo, S.J. Pachuta, R.G. Cooks, Soft-landing of polyatomic ions at fluorinated self-assembled monolayer surfaces, Science 275 (1997) 1447–1450.
[72] H. Luo, S.A. Miller, R.G. Cooks, S.J. Pachuta, Soft landing of polyatomic ions for selective modification of fluorinated self-assembled monolayer surfaces, Int. J. Mass Spectrom. Ion Process. 174 (1998) 193–217.
[73] H. Usui, Polymeric film deposition by ionization-assisted method for optical and optoelectronic applications, Thin Solid Films 365 (2000) 22–29.
[74] M.B.J. Wijesundara, L. Hanley, B. Ni, S.B. Sinnott, Effects of unique ion chemistry on thin-film growth by plasma–surface interactions, Proc. Nat. Acad. Sci. USA 97 (2000) 23–27.
[75] M.B.J. Wijesundara, Y. Ji, B. Ni, S.B. Sinnott, L. Hanley, Quantifying the effect of polyatomic ion structure on thin-film growth: experiments and molecular dynamics simulations, J. Appl. Phys. 88 (2000) 5004–5016.
[76] L. Diederich, E. Barborini, P. Piseri, A. Podesta, P. Milani, A. Schneuwly, R. Gallay, Supercapacitors based on nanostructured carbon electrodes grown by cluster-beam deposition, Appl. Phys. Lett. 75 (1999) 2662.
[77] V. Paillard, P. Melinon, V. Dupuis, A. Perez, J.P. Perez, G. Guiraud, J. Fornazero, G. Panczer, Production of diamondlike carbon films through random compact cluster stacking, Phys. Rev. B 49 (1994) 11433.
[78] W. Christen, U. Even, Collisional energy loss in cluster surface impact: experimental, model, and simulation studies of some relevant factors, J. Phys. Chem. A 102 (1998) 9420.
[79] D. Donadio, L. Colombo, P. Milani, G. Benedek, Growth of nanostructured carbon films by cluster assembly, Phys. Rev. Lett. 83 (1999) 776.
[80] L. Qi, S.B. Sinnott, Polymerization via cluster–solid surface impacts—molecular dynamics simulations, J. Phys. Chem. B 101 (1997) 6883–6890.
[81] L. Qi, S.B. Sinnott, Effect of cluster size on the reactivity of organic molecular clusters: atomistic simulations, Nucl. Instrum. Meth. Phys. Res. B 140 (1998) 39–46.
[82] L. Qi, W.L. Young, S.B. Sinnott, Effect of surface reactivity on the nucleation of hydrocarbon thin films through molecular-cluster beam deposition, Surf. Sci. 426 (1999) 83–91.
[83] L. Qi, S.B. Sinnott, Generation of 3D hydrocarbon thin films via organic molecular cluster collisions, Surf. Sci. 398 (1998) 195–202.
[84] S.K. Ghandhi, VLSI Fabrication Principles: Silicon and Gallium Arsenide, second ed., Wiley, New York, 1994.
[85] E.J.H. Collart, K. Weemers, D.J. Gravesteijn, J.G.M. van Berkum, Characterization of low-energy (100–10 keV) boron ion implantation, J. Vac. Sci. Technol. B 16 (1998) 280–285.
[86] W.L. Harrington, C.W. Magee, M. Pawlik, D.F. Downey, C.M. Osburn, S.B. Felch, Techniques and applications of secondary ion mass spectrometry and spreading resistance profiling to measure ultrashallow junction implants down to 0.5 keV B and BF_2, J. Vac. Sci. Technol. B 16 (1998) 286–291.
[87] C.L. Hartford, R.J. Hillard, R.G. Mazur, M.A. Foad, High-resolution damage depth profiles of unannealed sub-100 nm B^+ implants in (100) silicon, J. Vac. Sci. Technol. B 16 (1998) 316–319.
[88] M. Sosnowski, The prospects for low energy implantation with large molecular ions—the case of decaborane, Proc. 15th Int. Conf. Appl. Accelerators Res. Ind., Denton, TX, 1998, AIP Conf. Proc., p. 475, 775.
[89] R. Smith, M. Shaw, R.P. Webb, M.A. Foad, Ultrashallow junctions in Si using decaborane? A molecular dynamics simulations study, J. Appl. Phys. 83 (1998) 3148–3152.
[90] M.A. Foad, R. Webb, R. Smith, J. Matsuo, A. Al-Bayati, T. Shen-Wang, T. Cullis, Shallow junction formation by decaborane molecular ion implantation, J. Vac. Sci. Technol. B 18 (2000) 445–449.
[91] J.W. Coburn, Surface-science aspects of plasma-assisted etching, Appl. Phys. A 59 (1994) 451–458.
[92] S.S. Todorov, E.R. Fossum, Growth mechanism of thin oxide films under low-energy oxygen-ion bombardment, J. Vac. Sci. Technol. B 6 (1988) 466.
[93] C.L. Quinteros, T. Tzvetkov, D.C. Jacobs, Eley-Rideal reaction of O^+ with oxidized Si(100), J. Chem. Phys. 113 (2000) 5119.
[94] C.T. Rettner, Dynamics of the direct reaction of hydrogen atoms adsorbed on Cu(111) with hydrogen atoms

incident from the gas phase, Phys. Rev. Lett. 69 (1992) 383.
[95] S.A. Ruatta, E. Smith, A. Yasako, Advanced photomask reconstruction with the Seiko SIR 3000, 17th Annual BACUS Symposium on Photomask Technology Management, Redwood City, CA, 1987.
[96] M.J. Vasile, L.R. Harriot, Focused ion beam stimulated deposition of organic compounds, J. Vac. Sci. Technol. B 7 (1989) 1954–1958.
[97] E.T. Ada, L. Hanley, S. Etchin, J. Melngailis, W.J. Dressick, M.-S. Chen, J.M. Calvert, Ion beam modification and patterning of organosilane self-assembled monolayers, J. Vac. Sci. Technol. B 13 (1995) 2189–2196.
[98] J.S. Huh, M.I. Shepard, J. Melngailis, Focussed ion beam lithography, J. Vac. Sci. Technol. B 9 (1991) 173–175.
[99] E.H. Lee, Ion-beam modification of polymeric materials—fundamental principles and applications, Nucl. Instrum. Meth. Phys. Res. B 151 (1999) 29–41.
[100] E.H. Lee, M.B. Lewis, P.J. Blau, L.K. Mansur, Improved surface properties of polymer materials by multiple ion beam treatment, J. Mater. Res. 6 (1991) 610.
[101] G.R. Rao, E.H. Lee, Effects of sequential He^+ and Ar^+ implantation on surface properties of polymers, J. Mater. Res. 11 (1996) 2661.
[102] E.H. Lee, Y. Lee, W.C. Oliver, L.K. Mansur, Hardness measurements of Ar^+ beam treated polyimide by depth-sensing ultralow load indentation, J. Mater. Res. 8 (1993) 377.
[103] D.W. Brenner, O. Shenderova, C.B. Parker, Ion beam damage of polymer surfaces: insights from molecular-dynamics simulations, Materials Research Society, Pittsburgh, PA, 1997.
[104] K. Beardmore, R. Smith, Ion bombardment of polyethylene, Nucl. Instrum. Meth. Phys. Res. B 102 (1995) 223.
[105] D.M. Ròck, D. Boos, I.G. Brown, Improvement in wear characteristics of steel tools by metal ion implantation, Nucl. Instrum. Meth. Phys. Res. B 80/81 (1993) 233.
[106] R.J. Rodriguez, A.L. Sanz, A.M. Medrano, The search for new applications of ion implantation treatments, Surf. Coat. Technol. 84 (1996) 594.
[107] N.J. Mikkelsen, S.S. Eskildsen, C.A. Straede, N.G. Chechenin, Formation of low friction and wear-resistant carbon coatings on tool steel by 75 keV, high dose carbon ion implantation, Surf. Coat. Technol. 65 (1994) 154.
[108] J. Sasaki, K. Hayashi, K. Sugiama, O. Ichico, Y. Hashiguchi, Implantation of titanium, chromium, yttrium, molybdenum, silver, hafnium, tantalum, tungsten, and platinum ions generated by a metal vapor deposition source into 440C stainless steel, Surf. Coat. Technol. 51 (1992) 166.
[109] F. Alonso, J.L. Viviente, J.I. Onate, B. Torp, B.R. Nelsen, Effects of implantation treatments on micromechanical properties of M2 steel, Nucl. Instrum. Meth. Phys. Res. B 80/81 (1993) 254.
[110] C.A. Straede, N.J. Mikkelsen, Industrial implementation of ion implantation on tools and wear parts based on a strategic approach, Surf. Coat. Technol. 103–104 (1998) 191.
[111] F. Alonso, A. Garcia, J.J. Ugarte, J.L. Viviente, J.I. Onate, P.S. Baranda, C.V. Cooper, Changes in tribological properties of AISI 440C martensitic stainless steel after ion implantation of carbon at very high doses, Surf. Coat. Technol. 83 (1996) 263.
[112] S. Yan, W.J. Zhao, D.M. Ròck, J.M. Xue, Y.G. Wang, Study of tribological properties of high-speed steel implanted by high-dose carbon ions, Surf. Coat. Technol. 103–104 (1998) 348.
[113] F. Jhrling, D.M. Ròck, H. Fuess, Hardness, wear and microstructure of carbon implanted AISI M2 high speed steel, Surf. Coat. Technol. 111 (1999) 111.
[114] P.J. Evens, T. Vilaithong, L.D. Yu, O.R. Monteiro, K.M. Yu, I.G. Brown, Tribological effects of oxygen ion implantation into stainless steel, Nucl. Instrum. Meth. Phys. Res. B 168 (2000) 53.
[115] J. Sasaki, K. Hayashi, K. Sugiyama, O. Ichiko, Y. Hashiguchi, Changes in friction characteristics and microstructure of steel by ion implantation of titanium and additional carbon in various doses (I), Surf. Coat. Technol. 65 (1994) 160.
[116] K. Hayashi, J. Sasaki, K. Sugiyama, O. Ichiko, K. Tanaka, Y. Hashiguchi, Changes in friction characteristics and microstructure of steel by ion implantation of titanium and additional carbon in various doses (II), Surf. Coat. Technol. 65 (1994).
[117] N. Dytlewski, P.J. Evans, I.G. Brown, F. Liu, E.M. Oks, G.Y. Yushkov, Time-of-flight ERDA of dual implanted metals, Nucl. Instrum. Meth. Phys. Res. B 136–138 (1998) 644.
[118] J.I. Othate, F. Alonso, J.L. Viviente, A. Arizaga, A study of dual chromium plus carbon ion implantation into high speed steel, Surf. Coat. Technol. 65 (1994) 165.
[119] V. Paillard, P. Melinon, V. Dupuis, J.P. Perez, A. Perez, B. Champagnon, Diamondlike carbon films obtained by low energy cluster beam deposition: evidence of a memory effect of the properties of free carbon clusters, Phys. Rev. Lett. 71 (1993) 4170.
[120] R.C. Mowrey, D.W. Brenner, B.I. Dunlap, J.W. Mintmire, C.T. White, Simulations of C_{60} collisions with a hydrogen-terminated diamond 111 surface, J. Chem. Phys. 95 (1991) 7138.
[121] E.E.B. Campbell, I.V. Hertel, Hyperthermal chemistry and cluster collisions, Nucl. Instrum. Meth. Phys. Res. B 112 (1996) 48.
[122] H.-P. Cheng, Cluster–surface collisions: characteristics of Xe_{55}- and C_{20}-Si(111) surface bombardment, J. Chem. Phys. 111 (1999) 7583.
[123] M. Kerford, R.P. Webb, An investigation of the thermal profiles induced by energetic carbon molecules on a graphite surface, Carbon 37 (1999) 859.
[124] G. Brauchle, S. Richard-Schneider, D. Illig, R.D. Beck, H. Schreiber, M.M. Kappes, STM investigation of

energetic carbon cluster ion penetration depth into HOPG, Nucl. Instrum. Meth. Phys. Res. B 112 (1996) 105.
[125] T. Nohmi, J.B. Fenn, Electrospray mass spectrometry of poly(ethylene glycols) with molecular weights up to five million, J. Am. Chem. Soc. 114 (1992) 3241–3246.
[126] C.T. Reimann, R.A. Sullivan, J. Axelsson, A.P. Quist, S. Altmann, P. Roepstorff, I. Velazquez, O. Tapia, Conformation of highly-charged gas-phase lysozyme revealed by energetic surface imprinting, J. Am. Chem. Soc. 120 (1998) 7608–7616.
[127] L. Hanley, H. Lim, D.G. Schultz, S. Garbis, C. Yu, E.T. Ada, M.B.J. Wijesundara, Energetics, timescales and chemistry of low energy molecular ion–organic surface collisions, Nucl. Instrum. Meth. Phys. Res. B 157 (1999) 174–182.
[128] M.B.H. Breese, Focused MeV ion neams for materials analysis and microfabrication, Mater. Res. Soc. Bull. 25 (2000) 11.
[129] S. Rusponi, G. Costantini, F. Buatier de Mongeot, C. Boragno, U. Valbusa, Patterning a surface in the nanometric scale by ion sputtering, Appl. Phys. Lett. 75 (1999) 3318–3320.
[130] J.R. Hahn, H. Kang, Spatial distribution of defects generated by hyperthermal Ar^+ impact onto graphite, Surf. Sci. 446 (2000) L77–L82.
[131] A. Arnau, F. Aumayr, P.M. Echenique, M. Grether, W. Heiland, J. Limburg, R. Morgenstern, P. Roncin, S. Schippers, R. Schuch, et al., Interaction of slow multicharged ions with solid surfaces, Surf. Sci. Rep. 27 (1997) 113–239.
[132] S. Netcheva, P. Bertrand, Surface topography development of thin polystyrene films under low energy ion irradiation, Nucl. Instrum. Meth. Phys. Res. B 151 (1999) 129–134.
[133] F. Machalett, K. Edinger, L. Ye, J. Melngailis, T. Venkatesan, M. Diegel, K. Steenbeck, Focused-ion beam writing of electrical connections into platinum oxide films, Appl. Phys. Lett. 76 (2000) 3445–3447.
[134] J. Gierak, E. Cambril, M. Schneider, C. David, D. Mailly, J. Flicstein, G. Schmid, Very high-resolution focused ion beam nanolithography improvement: a new three-dimensional pattering capability, J. Vac. Sci. Technol. B 17 (1999) 3132–3136.
[135] P. Ruchhoeft, M. Colburn, B. Choi, H. Nounu, S. Johnson, T. Bailey, S. Damle, M. Stewart, J. Ekerdt, S.V. Sreenivasan, et al., Patterning curved surfaces: template generation by ion imprint proximity lithography and relief transfer by step and flash imprint lithography, J. Vac. Sci. Technol. B 17 (1999) 2965.
[136] B. Jandeleit, D.J. Schaefer, T.S. Powers, H.W. Turner, W.H. Weinberg, Combinatorial materials science and catalysis, Angew. Chem. Int. Ed. 38 (1999) 2494–2532.
[137] R.B. van Dover, L.F. Schneemeyer, R.M. Fleming, Discovery of a useful thin-film dielectric using a composition-spread approach, Nature 392 (1998) 162–164.
[138] B.D. Ratner, Biomaterials science: an interdisciplinary endeavor, in: B.D. Ratner, A.S. Hoffman, F.J. Schoen, J.E. Lemons (Eds.), Biomaterials Science: An Introduction to Materials in Medicine, Academic Press, New York, 1996, pp. 1–8.
[139] H. Zreiqat, P. Evans, C.R. Howlett, The effect of surface chemical modification of bioceramic on phenotype of human bone-derived cells, J. Biomed. Mater. Res. 44 (1999) 389–396.
[140] C. Satriano, G. Marletta, E. Conte, Cell adhesion on low-energy ion beam-irradiated polysiloxane surfaces, Nucl. Instrum. Meth. Phys. Res. B 148 (1999) 1079–1084.
[141] A.A. Bergman, J. Buijs, J. Herbig, D.T. Mathes, J.J. Demarest, C.D. Wilson, C.T. Reimann, R.A. Baragiola, R. Hull, S.O. Oscarsson, Nanometer-scale arrangement of human serum albumin by adsorption on defect arrays created with a finely focused ion beam, Langmuir 14 (1998) 6785–6788.
[142] X. Cheng, D.G.I. Camp, Q. Wu, R. Bakhtiar, D.L. Springer, B.J. Morris, J.E. Bruce, G.A. Anderson, G.G. Edmonds, R.D. Smith, Molecular weight determination of plasmid DNA using electrospray ionization mass spectrometry, Nucl. Acids Res. 24 (1996) 2183–2189.
[143] C.J. Buchko, K.M. Kozloff, A. Sioshansi, K.S. O'Shea, D.C. Martin, Electric field mediated deposition of bioactive polypeptides on neural prosthetic devices, Mat. Res. Soc. Symp. Proc. 414 (1996) 23–28.
[144] B. Feng, D.S. Wunschel, L.P. Tolic, R.D. Smith, ESI-FTICR analysis and recovery of DNA and PCR products through soft-landing, 46th ASMS Conf. Mass Spectrom. Allied Topics, Orlando, FL, 1998.
[145] Y. Xia, R.J. Geiger, M.G. Bartlett, K.L. Busch, Soft-landing of biological compounds using a beam mass spectrometer, 46th ASMS Conf. Mass Spectrom. Allied Topics, Orlando, FL, 1998.
[146] V.N. Morozov, T.Y. Morozova, Electrospray deposition as a method for mass fabrication of mono- and multicomponent microarrays of biological and biologically active substances, Anal. Chem. 71 (1999) 3110–3117.
[147] F. Charbonnier, L. Berthelot, C. Rolando, Differentiating between capillary and counter electrode processes during electrospray ionization by opening the short circuit at the collector, Anal. Chem. 71 (1999) 1585–1591.
[148] J.W. Rabalais, A.H. Al Bayati, K.J. Boyd, D. Marton, J. Kulik, Z. Zhang, W.K. Chu, Ion-energy effects in silicon ion-beam epitaxy, Phys. Rev. B 53 (1996) 10781–10792.
[149] S.S. Todorov, H. Bu, K.J. Boyd, J.W. Rabalais, C.M. Gilmore, J.A. Sprague, Ion beam deposition of Ag-107(111) films on Ni(100), Surf. Sci. 429 (1999) 63–70.
[150] D.C. Jacobs, The role of internal energy and approach geometry in molecule/surface reactive scattering, J. Phys. Condens. Matter 7 (1995) 1023.
[151] M.B.J. Wijesundara, E. Fuoco, L. Hanley, Preparation of chemical gradient surfaces by hyperthermal polyatomic ion-deposition: A new method for combinatorial materials science, Langmuir 17 (2001) 5721–5726.